NANO LETTERS

Letter

pubs.acs.org/NanoLett

Novel Scheme for Producing Nanoscale Uniform Grains Based on Templated Two-Phase Growth

Vignesh Sundar,*[,†,‡] Jingxi Zhu,*[,§,∥] David E. Laughlin,[†,‡,⊥] and Jian-Gang (Jimmy) Zhu[†,‡,⊥]

[†]Data Storage Systems Center, Carnegie Mellon University, Pittsburgh, Pennsylvania 15213, United States

[‡]Department of Materials Science and Engineering, Carnegie Mellon University, Pittsburgh, Pennsylvania 15213, United States

[§]Sun Yat-sen University−Carnegie Mellon University Joint Institute of Engineering, Sun Yat-sen University, Guangzhou, China

[∥]Sun Yat-sen University−Carnegie Mellon University Shunde International Joint Research Institute, Sun Yat-sen University, Guangdong, China

[⊥]Department of Electrical and Computer Engineering, Carnegie Mellon University, Pittsburgh, Pennsylvania 15213, United States

ABSTRACT: Future magnetic recording media require firm control of the microstructure particularly with uniform grain size at the nanometer scale. Using self-assembling block copolymers as an etch-mask, a novel underlayer is patterned with a carefully designed surface morphology. Two-phase growth with magnetic grains encircled by an oxide phase is guided by the templated underlayer to create high-coercivity magnetic media with uniform grain size at the nanoscale.

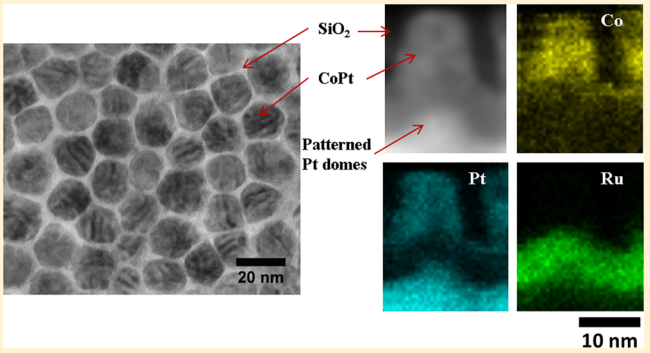

KEYWORDS: *Magnetic recording media, block copolymers, uniform grain size, templated growth*

In order to meet the ever-increasing demand for higher data storage capacities, extensive research has been performed for improving the current perpendicular magnetic media,[1] while the development of next-generation technologies such as heat-assisted magnetic recording[2] and bit-patterned media[3] is underway. From a materials perspective, control of the thin film microstructure is crucial for enabling and improving these technologies. In the case of current perpendicular media based on CoCrPt-SiO_2 with a granular microstructure, minimizing distributions in grain size and grain boundary segregant thickness will aid further reduction in transition noise and improve the signal-to-noise ratio.[4,5]

In present hard disk drives, the recording medium is a thin magnetic film (about 12 nm in thickness) consisting of a single layer of magnetic grains (about 8 nm in diameter) which are separated by a nonmagnetic oxide phase at their grain boundaries. Each magnetic grain is a single crystal of the CoCrPt alloy which has the hexagonal close packed (HCP) structure and the *c*-axis is oriented perpendicular to thin film plane. The HCP CoCrPt crystalline grains have strong uniaxial magnetocrystalline anisotropy with their easy axes parallel to their *c*-axes. The oxide at their boundaries serve the purpose of cutting off the exchange coupling between neighboring grains, which is critical to the desired recording performance, especially for high storage area densities.[7] This granular microstructure is created by epitaxial growth of the CoCrPt-oxide layer on a ruthenium (Ru) underlayer, which also has the HCP structure and (0002) texture. The top portion of the Ru underlayer is usually deposited at a relatively high Ar pressure by sputtering, with each Ru grain forming dome-shape surface topology, critical for yielding the microstructure of the magnetic layer on top.[6]

At sub-10 nm dimensions, each magnetic grain is a single storage entity since magnetization within them is essentially uniform. The storage fidelity of each stored data bit, that is, the corresponding signal-to-noise ratio in read-back, is directly proportional to the number of magnetic grains with which the bit is comprised. In addition, the grain size distribution is also critical. At 8 nm grain size, the anisotropy energy of each grain is approximately 80−100 times the thermal energy (k_BT) at ambient temperature. Smaller size grains suffer significant thermal agitation, yielding an uncertainty of magnetization orientation both during recording and in long-term storage. Magnetic recording media currently has grain sizes of approximately 8 nm, with distributions of 26%.[8]

In this Letter, we report a coherent templated growth of magnetic recording media, enabling control of microstructure, potentially lowering grain size and grain boundary segregant distributions. This template consists of a prepatterned morphology of a suitable material. Growth of magnetic media, typically using sputtering, onto this template, results

Received: January 6, 2014
Revised: February 12, 2014

   dx.doi.org/10.1021/nl500061t | *Nano Lett.* XXXX, XXX, XXX−XXX

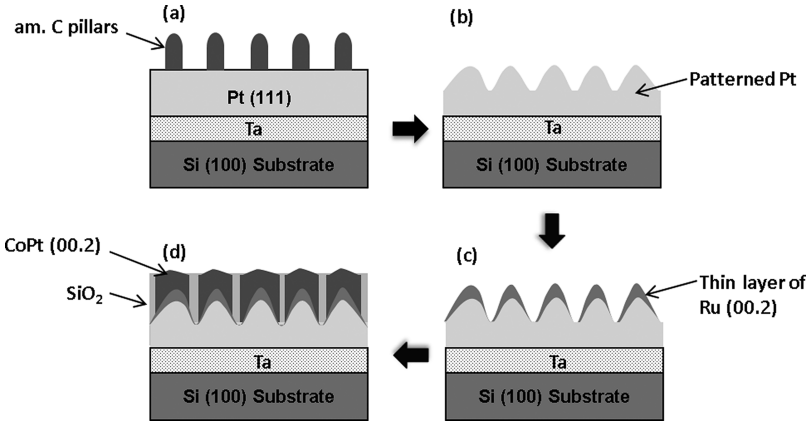

Figure 1. Illustration of process flow for fabrication of templated magnetic media showing film stack (a) after fabrication of am-C pillars, (b) after pattern transfer into template layer, (c) after sputtering underlayer, and (d) after sputtering magnetic layer with segregant.

in a microstructure defined by the sites on the template. For CoCrPt based magnetic media, platinum (Pt) is a suitable template material. Pt, having a face-centered cubic (FCC) crystal structure, favors film growth with (111) texture. In the (111) plane, the lattice mismatch with the (0002) plane of ruthenium (Ru), typically used as the underlayer in conventional magnetic recording media, is only 2.5%. Pt with (111) texture can thus be used as a template layer to grow Ru epitaxially with (0002) texture (Ru has a hexagonal close packed or HCP crystal structure). However, Pt cannot be used directly as underlayer for CoCrPt. In such a case, due to next-nearest neighbor interactions, CoCrPt starts to grow with the FCC (111) texture, in which it does not possess uniaxial magnetic anisotropy, and is thus not useful for magnetic recording. As discussed earlier, CoCrPt having a HCP (0002) texture, with high uniaxial magnetic anisotropy is required for magnetic recording applications. Another advantage of using Pt for template creation is its resistance to oxidation and retention of surface characteristics which result in good texture (with low rocking angle) of Ru even if the template is exposed to atmosphere. If instead, the template is created using Ru, the modified surface could result in poor texture of CoCrPt sputtered onto Ru, affecting the magnetic properties. In this work, $Co_{84}Pt_{16}$ alloy was used as the magnetic material, and forms a HCP structure with high uniaxial anisotropy as described earlier, with SiO_2 as the segregant.

A 3 nm amorphous Ta layer was first sputtered to improve adhesion between a 1″ Si substrate (with native oxide), and the sputtered Pt. A 15 nm template layer of Pt was then sputtered with conditions optimized to obtain FCC (111) texture with a low rocking angle of 4°. Pt and Ta were sputtered using DC sputtering at rates of 7.8 and 9 nm/min using a 5-target Nanofab sputtering system at an Ar pressure of 2.5 mT.

An overview of the templated media growth process is shown in Figure 1. A hexagonal array of pillars is first fabricated in a suitable hard mask such as amorphous carbon as shown in Figure 1a. This pattern is then used to fabricate domes in the template material (Pt), by ion-milling (Figure 1b). After sputtering a thin layer of Ru to obtain the desired HCP (0002) texture (Figure 1c), CoPt-SiO_2 is sputtered from a composite target (Figure 1d), and it is found that the CoPt grows on top of the domes defined by the template, while SiO_2 goes into the trenches.

Patterning of the hard mask is achieved using self-assembling block copolymers (BCP). Diblock copolymers consist of "blocks" of homopolymers which are energetically incompatible with each other and hence phase-separate. Since the chains are connected by a covalent bond, the phase-separation occurs on a microscale. The phase-segregating tendency of the block copolymers is related to the product of the Flory–Huggins parameter χ and the degree of polymerization.[9] Furthermore, microphase separated block copolymer domains can be "guided" to obtain long-range ordering.[10−12] Block copolymer lithography has been shown as a promising candidate for achieving feature sizes which are not accessible with high throughput using current lithography techniques.[13] For this work, silicon containing block copolymer poly(styrene-*b*-dimethylsiloxane) (PS-*b*-PDMS) was used, in view of the following advantages: it has a high χ value, thus potentially enabling sub-10 nm feature sizes, and high etch-selectivity in reactive ion etching process facilitating pattern transfer into underlying layers.[14] PS-*b*-PDMS (13.8 kg mol^{-1}, f_{PDMS} = 0.16, PDI = 1.14) was purchased from Polymer Source Inc. For such a volume fraction, spheres of PDMS in a polystyrene matrix were obtained upon microphase separation. Before spin-coating the polymer film, 20 nm of amorphous carbon (referred to as am-C from hereon) (to be used as hard mask) was DC sputtered onto the film stack at a rate of 2 nm/min with an Ar pressure of 5 mT. Then, from a 0.35 wt/wt % solution of the polymer in toluene, a thin film of BCP was spin-coated onto the film stack using dynamic dispense technique, with a spin speed of 6200 rpm. Solvent annealing was then performed at room temperature using 0.05 mL of toluene for 14 h to facilitate microphase separation. The thin PDMS layer that segregated to the top was first etched using a CF_4 plasma in a Plasma-Therm 790 Reactive Ion Etching system, followed by a low-bias (~65 V) O_2 plasma etch to selectively etch out the polystyrene matrix.[14] During this process, the PDMS spheres were partially oxidized and could be used as an etch-mask to transfer the pattern using O_2 plasma into the underlying am-C hard mask. Figure 2 shows a plane-view scanning electron micrograph of patterned am-C hard mask, imaged in a FEI Sirion 600 SEM operated at 10 kV using a through-the-lens ultrahigh resolution detector at a working distance of 4 mm. The average center-to-center distance between the am-C pillars is 17.3 nm, with a standard deviation of 14%.

The pattern was then transferred into the Pt layer using a Commonwealth Scientific ion mill with a 16 cm Kaufmann ion-source at a bias of 500 V and a current of 40 mA to pattern the Pt layer. The substrate was tilted such that the normal to the

dx.doi.org/10.1021/nl500061t | *Nano Lett.* XXXX, XXX, XXX−XXX

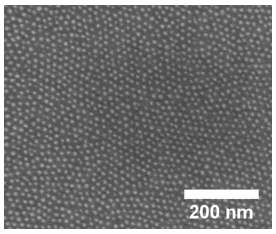

Figure 2. Plane-view scanning electron micrograph of am-C pillars after reactive ion etching.

plane was at an angle of 12.5° to the ion beam and was rotated to ensure uniform milling. 6 nm of Ru was then deposited onto this template using RF sputtering, at an Ar pressure of 5 mT and rate of 4.8 nm/min. Without breaking vacuum, 10 nm of CoPt-SiO_2 was then deposited from a composite target at an argon pressure of 45 mT, with a rate of approximately 10 nm/min.

The effect of this templating process on the magnetic properties of the media was characterized using a Princeton Alternating Gradient Force magnetometer. To understand the effect of templating, a sample was made where the Pt layer was not patterned. The conditions and thickness for the deposition of Ru and CoPt-SiO_2 were kept the same. From the out-of-plane magnetic hysteresis loops for the templated and the untemplated samples (shown in Figure 3a), we see that the templated sample has a much higher coercivity of approximately 5 kOe, but there is also a lowering of the remanent magnetization. The higher coercivity can be attributed to better exchange decoupling between the magnetic grains as described earlier in our discussion of the film microstructure. We are still investigating the probable causes for the lowering of the remanent magnetization, but it is likely due to contribution from regions in the sample where the block copolymer pattern was poorly defined. In contrast, we see that the reference sample had a very low coercivity due to higher exchange coupling between the CoPt grains. The templating process also seems to aid the improvement of the uniaxial anisotropy. From the in-plane hysteresis loops (shown in Figure 3b), the field at which the sample saturates is a good measure of the anisotropy field of the sample, which can be written as $H_k = H_s + N_d M_s$, where H_k is the magnetic anisotropy field, H_s is the saturation field for in-plane measurement, N_d is the demagnetization factor, and M_s is the saturation magnetization of the material. Further, the uniaxial anisotropy constant can then be estimated as $K_u = M_s H_k/2$. We find that the templated CoPt film had a much higher K_u of 7.7×10^6 erg/cm^3 (as compared to 6.5×10^6 for the untemplated sample). Since the thermal stability of data is determined by the product of K_u and the volume of the grain, a higher K_u is a desirable property. On the other hand, there is a nonzero remanent magnetization in the in-plane curve, indicating the presence of a small percentage of magnetic grains with in-plane orientation. This could again be the effect of regions of the film where the block copolymer pattern is poorly defined, and we are further investigating how to improve this aspect of the magnetic properties.

The plane-view transmission electron micrograph for the templated magnetic media is shown in Figure 4, taken using a JEOL JEM-2000EX transmission electron microscope. From this bright field image, we can clearly see the CoPt grains surrounded by the lighter-appearing amorphous SiO_2. The average grain size of the CoPt grains is found to be 16.2 nm with a standard deviation of 11%. The grain size is thus defined by the center-to-center distance between the polymer spheres in the BCP pattern, which was earlier mentioned to be 17.2 nm. The difference in these numbers is indicative of the thickness of the SiO_2 grain boundaries. The distribution in grain size is also approximately the same as the distribution in the center-to-center spacings in the polymer pattern. By further optimizing the BCP patterning, these distributions can be further minimized, and this would translate to the magnetic media microstructure as a more uniform grain size. The fringes observed in Figure 4 result from the Moiré effect, which occur due to the interference of the diffracted beams from the CoPt

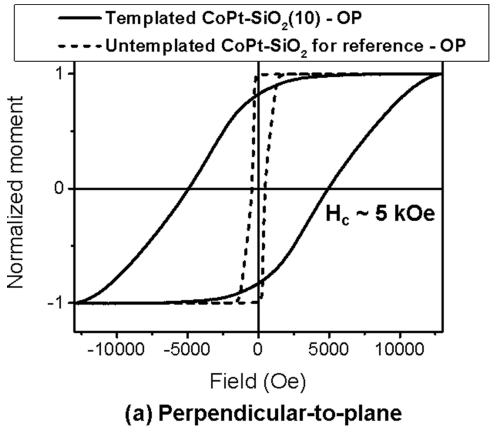

Figure 3. (a) Out-of-plane and (b) in-plane magnetic hysteresis loops for templated (solid line) and untemplated (dashed line) CoPt-SiO_2 magnetic media.

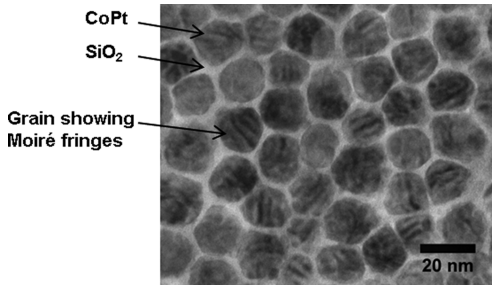

Figure 4. Plane-view transmission electron micrograph of templated CoPt-SiO_2 magnetic media.

dx.doi.org/10.1021/nl500061t | Nano Lett. XXXX, XXX, XXX−XXX

layer and the underlying Ru layer. The spacing of these fringes was measured to be 3.4 ± 0.2 nm, which roughly corresponds to the spacing expected for $\{11\bar{2}0\}$ planes.[15]

Scanning transmission electron microscopy (STEM) was used to study the cross-section microstructure of the templated media in a Philips Tecnai F20 FEG TEM fitted with a high-angle annular dark field (HAADF) detector. The specimen was prepared using a Nova 600 DualBeam (focused ion beam/electron beam) microscope by an in situ lift-out method. The specimen was first polished using a 30 kV focused Ga^+ beam at a current of 0.1 nA and cleaned with a 10 kV ion beam at a current of 30 pA. The HAADF-STEM image is shown in Figure 5a. In HAADF mode, the contrast observed is mostly due to

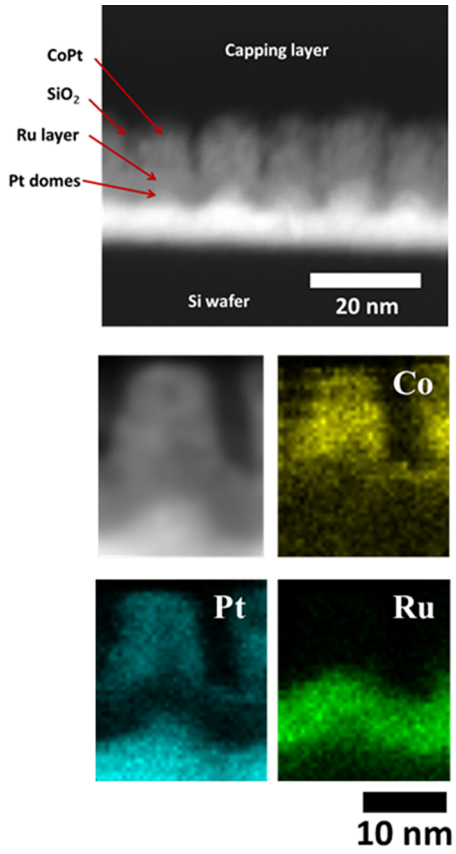

Figure 5. (a) High-angle annular dark field scanning transmission electron micrograph of templated CoPt-SiO_2 magnetic media. (b) EDS integrated intensity maps of Co, Pt, and Ru for one grain.

atomic number or "Z" contrast. Thus, as seen in Figure 5a, Pt, which has the highest "Z" among the materials in the sample, has the highest brightness. CoPt and Ru have similar contrast since the signal from Co and Pt is averaged. SiO_2 appears the darkest, and it is evident from the image that it goes between the domes, while the CoPt grows on the top of the domes as defined by the template.

Energy dispersive X-ray spectroscopy (EDS) was used to map the element distribution for one of the grains using a FEI Titan 80-300 TEM. Drift-corrected EDS spectra were collected at each point with a beam dwell time of 2 s. By selecting suitable X-ray peaks for each element, maps were then generated, where the brightness at a point corresponds to that element's relative concentration at that point. In the maps, we see the Pt domes demarcated clearly, with a continuous layer of Ru on top. The CoPt grain is also clearly outlined, and we see that it has grown on top of the dome. We were unable to map the location of Si or O due to poor signal-to-noise ratio in the EDS spectra, but considering the contrast in the HAADF image as well as the bright field plane-view images, it is evident that the SiO_2 is in-between the CoPt grains and in the trenches defined by the Pt domes. This is in agreement with the findings by groups who studied a dual-Ru underlayer for enabling granular microstructure of magnetic media, wherein the dome-morphology of Ru was created using high Ar pressure during sputtering, but with no control over the positions of these domes.[16,17]

We have thus been able to demonstrate a coherent, templated growth of magnetic media (CoPt + SiO_2) with a uniform grain size. This was achieved using domes patterned in a continuous Pt layer using block copolymer self-assembly. When magnetic media is sputtered onto it, the domes patterned in this template determine magnetic grain position, enabling control of magnetic film microstructure. Pt was appropriate as the template material due to its resistance to oxidation. In addition, it has a suitable crystallographic structure and can be grown with the right crystallographic texture to enable epitaxial growth of the subsequently deposited Ru and CoPt layers. The thin Ru layer was critical to obtain the right texture of the CoPt for it to be suitable for magnetic recording. Microstructural characterization using TEM, HAADF-STEM, and EDS mapping confirmed that the patterned domes acted as sites where the CoPt grains grew, while the SiO_2 went to the trenches. This was further supported by the magnetic hysteresis behavior comparison of the templated and untemplated samples. Since the grain positions are now guided by the patterned substrate, improvement in the block copolymer self-assembly process will lead to minimization of distributions in the pattern and thus in the magnetic media microstructure. Thus, for conventional magnetic recording, this technique could be used to reduce grain-size and grain-boundary thickness distributions resulting in better media performance. To utilize this technique for the fabrication of conventional magnetic recording media, it is necessary to further reduce the center-to-center spacing in the block copolymer pattern to ~10 nm features, shown to be possible by other groups.[18,19] The 10 nm feature patterns can also be obtained from nanoparticle lithography.[20] Another suitable application of this templated growth method is for the fabrication of bit patterned media. It is well-known that block copolymer domains can be ordered using topographical variations on the substrate or chemical prepatterning.[10,11,21,22] A combination of the templated growth technique outlined in this letter with long-range ordering of block copolymer domains could result in a technique for bit-patterned media fabrication where the magnetic material need not be etched (top-down approach), while also avoiding trench material (bottom-up approach) which may result in noise during recording.

AUTHOR INFORMATION

Corresponding Authors

*E-mail: vigneshs@andrew.cmu.edu.
*E-mail: jingxiz@andrew.cmu.edu.

Author Contributions

V.S., J.Z., D.E.L., and J.-G.Z. contributed equally.

Notes

The authors declare no competing financial interest.

dx.doi.org/10.1021/nl500061t | Nano Lett. XXXX, XXX, XXX−XXX

■ ACKNOWLEDGMENTS

The authors would like to thank Hoan Ho and Tom Nuhfer for assistance with transmission electron microscopy and Dr. Matthew Moneck and Dr. Bruce Terris for various fruitful discussions. This project was funded by through the Data Storage Systems Center of Carnegie Mellon University and its industrial sponsors.

■ REFERENCES

(1) Piramanayagam, S. N. *J. Appl. Phys.* **2007**, *102*, 011301.
(2) Weller, D.; Mosendz, O.; Parker, G.; Pisana, S.; Santos, T. S. *Phys. Status Solidi* **2013**, *210*, 1245−1260.
(3) Terris, B. D. *J. Magn. Magn. Mater.* **2009**, *321*, 512−517.
(4) Zhu, J.-G.; Sokalski, V.; Wang, Y.; Laughlin, D. E. *IEEE Trans. Magn.* **2011**, *47*, 74−80.
(5) Sokalski, V.; Laughlin, D. E.; Zhu, J.-G. *Appl. Phys. Lett.* **2009**, *95*, 102507.
(6) Piramanayagam, S. N.; Chong, T. C. *Developments in data storage: Materials perspective*; Wiley: New York, 2012.
(7) Zhu, J.-G.; Bertram, H. N. *J. Appl. Phys.* **1989**, *66*, 1291.
(8) Wang, T.; Mehta, V.; Ikeda, Y.; Do, H.; Takano, K.; Florez, S.; Terris, B. D.; Wu, B.; Graves, C.; Shu, M.; Rick, R.; Scherz, A.; Stöhr, J.; Hellwig, O. *Appl. Phys. Lett.* **2013**, *103*, 112403.
(9) Bates, F. S.; Fredrickson, G. H. *Annu. Rev. Phys. Chem.* **1990**, *41*, 525−557.
(10) Bita, I.; Yang, J. K. W.; Jung, Y. S.; Ross, C. A.; Thomas, E. L.; Berggren, K. K. *Science* **2008**, *321*, 939−943.
(11) Ruiz, R.; Kang, H.; Detcheverry, F. a; Dobisz, E.; Kercher, D. S.; Albrecht, T. R.; de Pablo, J. J.; Nealey, P. F. *Science* **2008**, *321*, 936−939.
(12) Hamley, I. W. *Prog. Polym. Sci.* **2009**, *34*, 1161−1210.
(13) Herr, D. J. C. *J. Mater. Res.* **2011**, *26*, 122−139.
(14) Jung, Y. S.; Ross, C. A. *Nano Lett.* **2007**, *7*, 2046−2050.
(15) Hossein-babaei, F.; Sinclair, R.; Srinivasan, K.; Bertero, G. A. *Nano Lett.* **2011**, *11*, 3751−3754.
(16) Shi, J. Z.; Piramanayagam, S. N.; Mah, C. S.; Zhao, H. B.; Zhao, J. M.; Kay, Y. S.; Pock, C. K. *Appl. Phys. Lett.* **2005**, *87*, 222503.
(17) Park, S. H.; Kim, S. O.; Lee, T. D.; Oh, H. S.; Kim, Y. S.; Park, N. Y.; Hong, D. H. *J. Appl. Phys.* **2006**, *99*, 08E701.
(18) Son, J. G.; Hannon, A. F.; Gotrik, K. W.; Alexander-Katz, A.; Ross, C. A. *Adv. Mater.* **2011**, *23*, 634−639.
(19) Park, S.; Lee, D. H.; Xu, J.; Kim, B.; Hong, S. W.; Jeong, U.; Xu, T.; Russell, T. P. *Science* **2009**, *323*, 1030−1033.
(20) Wen, T.; Booth, R. A.; Majetich, S. A. *Nano Lett.* **2012**, *12*, 5873−5878.
(21) Naito, K.; Hieda, H.; Sakurai, M.; Kamata, Y.; Asakawa, K. *IEEE Trans. Magn.* **2002**, *38*, 1949−1951.
(22) Stoykovich, M. P.; Nealey, P. F. *Mater. Today* **2006**, *9*, 20−29.